Journal of Engineering Physics and Thermophysics, Vol. 65, No. 3, 1993

FILM COOLING, MASS TRANSFER, AND FLOW AT THE BASE OF A TURBINE BLADE

M.Y. Jabbari and R.J. Goldstein

Studies of film cooling, mass transfer, and flow visualization near the endwall of a turbine blade of a fixed cascade are reviewed. Comparison of the results confirms the complex structure of the flow, including the existence of a number of interacting vortices that dominate the region. The film cooling and mass transfer variations are in correspondence with the observed flow structure.

INTRODUCTION

In recent years, considerable effort has been devoted to unravel the mysteries of the flow and heat transfer in gas turbines. Much has been learned from these investigations, but much more remains to be learned. To raise our understanding of key flow and transfer phenomena, a review is presented of some of the results of studies carried out at the University of Minnesota.

All the studies reviewed were made using a planar cascade which consists of six scaled-up turbine blades. A schematic of the cascade, the blades, and the relevant dimensions are given in Figure 1.

The instrumental section of the cascade includes the central passage and its bounding surfaces. Mass transfer techniques are employed in these investigations. For film cooling studies, a tracer gas is added to the injectant before its release into the mainstream boundary layer. Wall concentration of the tracer is then measured downstream of the injection port at preselected locations. Film cooling effectiveness is calculated from these measurements [1]. For heat transfer studies, the naphthalene sublimation technique is used. With this technique, the surface of interest is covered with a thin layer of naphthalene before it is exposed to a flow of air. Upon exposure, naphthalene sublimes and enters the air, causing local depressions (order of a hundredth of a millimeter) in the surface. Changes in the surface profile, measured relative to a datum, provides the amount of depression and is converted into a mass transfer coefficient (analogous to the corresponding heat transfer coefficient). An elaborate, computer-assisted data acquisition system [2] is used in the measurements of the surface profiles. A key strength of this approach is the ability to detect local maxima and minima in transport that are normally missed using other techniques. Visualization of the surface flow is accomplished employing a mixture of oil and lamp-black powder. A thin, smooth sheet of nonabsorbing contact paper is glued to the surface. A layer of well-mixed, freshly made mixture is thinly spread over the paper just before the flow of air is to start. Time is allowed for steady state flow to be established before the results are recorded. In interpreting the results, careful consideration is given to the possibility of washed-in accumulation of the mixture in a given area.

RESULTS AND DISCUSSION

Studies of film cooling performance for injection through a single row and two (staggered) rows of holes are reported in references [3, 4]. Measurements are taken on the blade's suction and pressure sides near and away from the endwall. With regard to the endwall effect, the pressure-side measurements do not show any significant change in the jet's performance except very close to the endwall $H/D < 10$. In this region, the effectiveness is generally lower, and the jets are skewed toward the endwall under the influence of the mainstream flow direction.

Mechanical Engineering Department, University of Minnesota, 111 Church Street SE, Minneapolis, MN 55455, USA. Published in Inzhenerno-Fizicheskii Zhurnal, Vol. 65, No. 3, pp. 350-355, September, 1993. Original article submitted May 22, 1992.

1062-0125/93/6503-0911$12.50

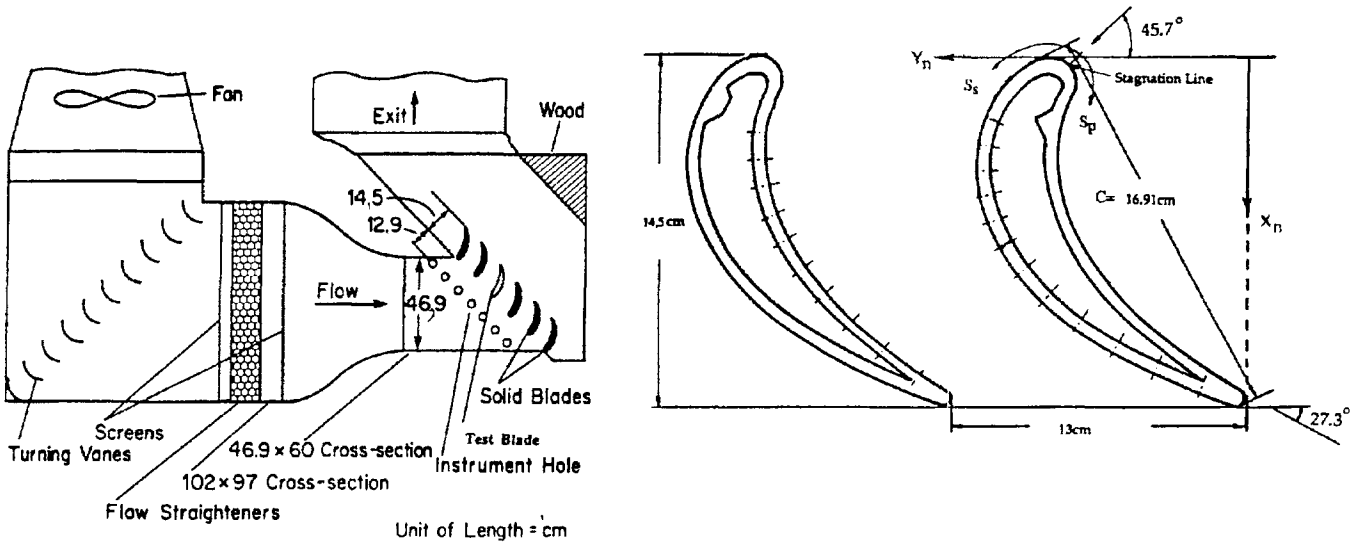

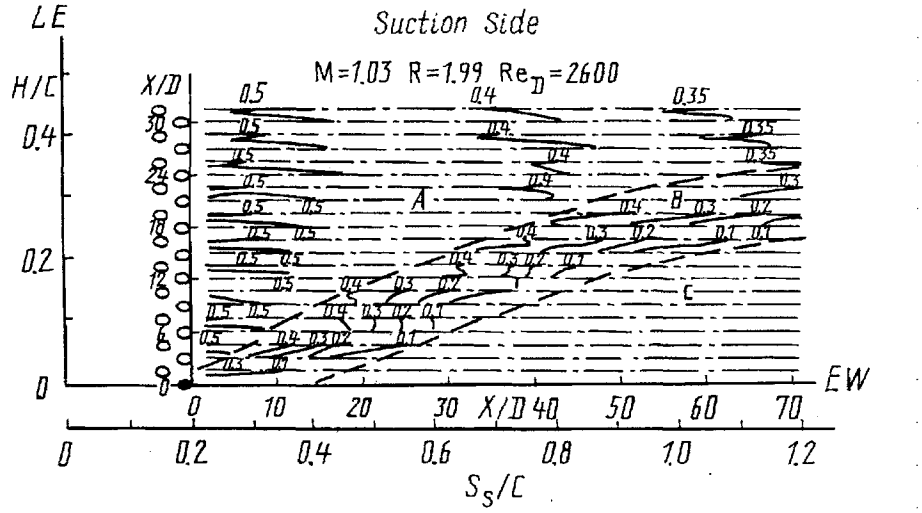

Fig. 1. Sketch of the cascade and the blades.

Fig. 2. Distribution of film cooling effectiveness on the suction side.

On the suction side, the endwall effect is quite pronounced. In Figure 2, iso-effectiveness contours of injection through two rows of holes are shown. Distribution of the contours, and their variation along the blade's span (H/D), indicate three distinct regions of film cooling protection. In a triangular region extending downstream from $S_s/C \simeq 0.4$ (labeled C), basically there is no film cooling protection. Above this region, in a strip labeled B, the film cooling effectiveness increases from a lower value at the border of region C to a higher value at the border of region A (approximate locations of the borders are shown by dashed lines). In region A, the effectiveness does not vary with changing H/D, and it assumes values equal to those measured far from the endwall. Similar variations are observed when a single row of injection holes is used. The shape and the extent of regions A, B, and C do not seem to be significantly altered by the film cooling parameters such as the blowing rate and the density ratio, either. These observations lead one to conclude that the performance of film cooling in region A is independent of the presence of endwall, and that in regions B and C, the endwall effect is governed only by the mainstream flow structure.

Mass transfer (naphthalene sublimation) measurements and flow visualization studies are carried out on the endwall and on the blade surfaces. Contours of Stanton number on the blade's suction side, determined from

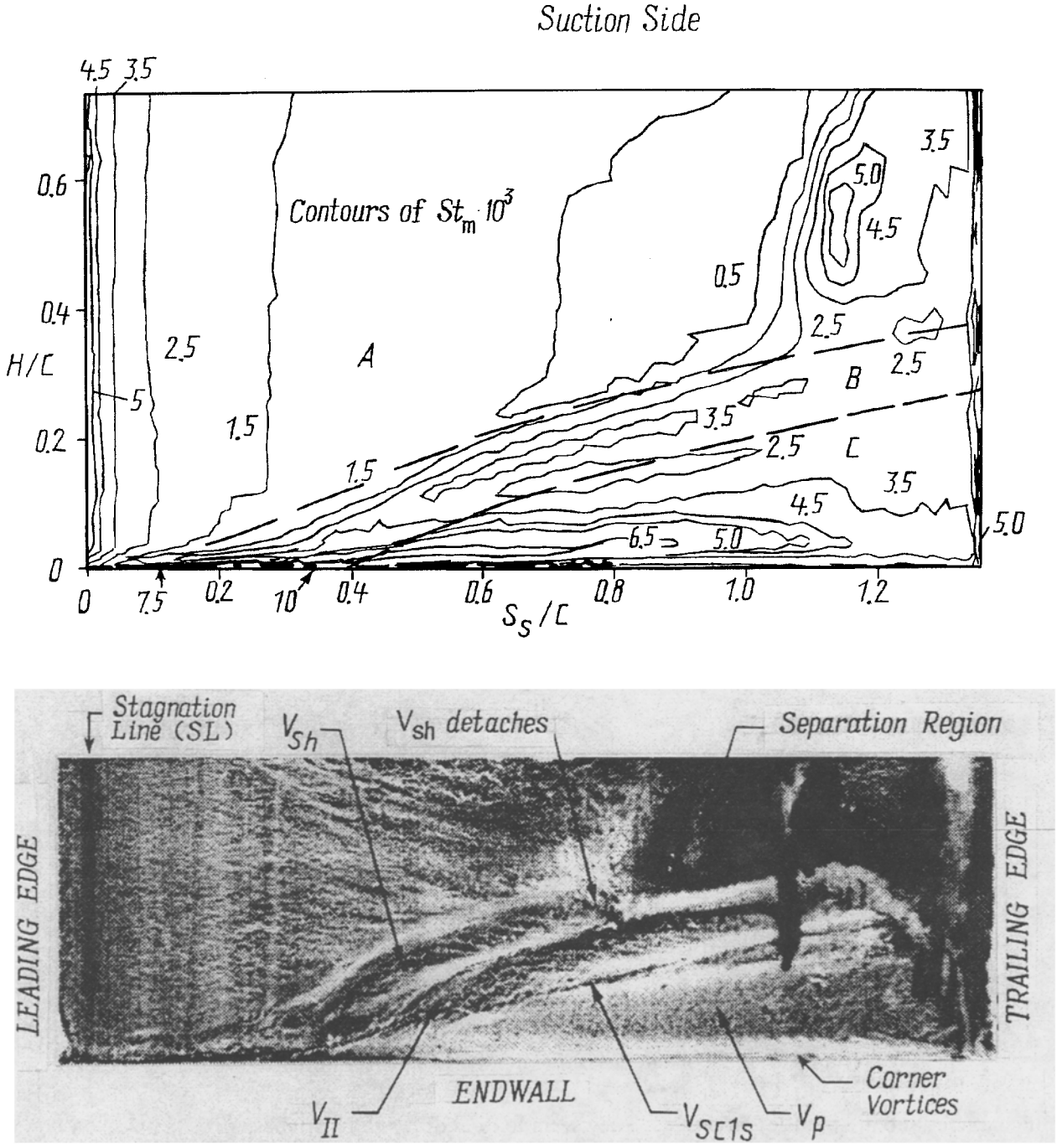

Fig. 3. Flow visualization and mass transfer distribution on the endwall.

measured mass transfer coefficients [5], are depicted in Figure 3. In the same figure, flow visualization results (using lamp-black technique) obtained on the same surface are also shown [6]. Several regions, having distinct density and alignment of lamp-black particles, are identifiable from the visualization. The difference in the region's particle texture indicates that different flow structures have existed immediately above the regions. Some similarities between the shape of iso-mass transfer contours and the boundaries of these regions are noticeable. Regions designated by A, B, and C in Figure 2 are clearly distinguishable in Figure 3 and are accordingly marked.

The results of mass transfer measurements on the endwall of the central passage [7] are shown in Figure 4. Lamp-black visualization of the surface flow in the same region is also included. Again, based on the density and alignment of the lamp-black particles, supported by the contours of Stanton number, several flow regions (sketched in the lower left-hand corner of the figure) are identified. Over these regions the near-surface flows have

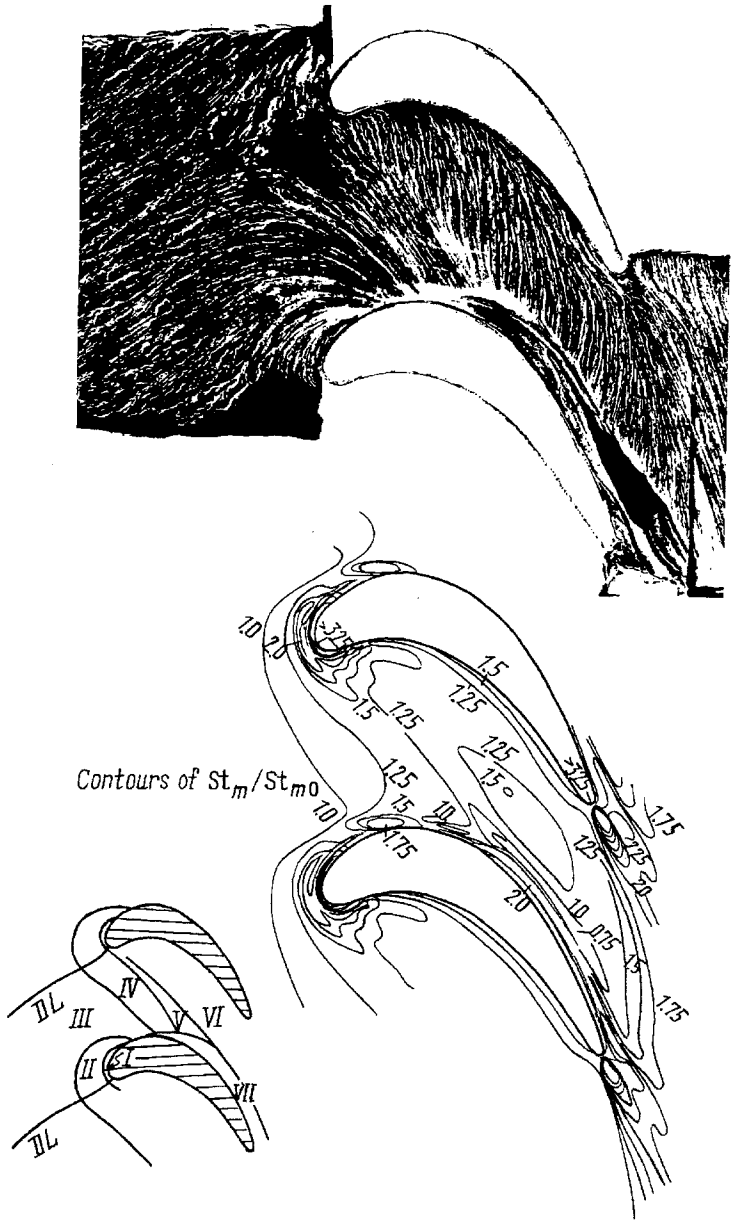

Fig. 4. Flow visualization and mass transfer distribution on the suction side.

different character and are of different origins. They seem to form different flow tubes. For example, the flow over region I constitutes the suction-side-leg of the horseshoe vortex with intense vertical motion; region II is covered by the slow moving fluid streaming out of the space occupied by the reversed flow ahead of the leading edge (the separation bubble); over region III flows the upstream fluid which has passed around the separation bubble and, consequently, has a relatively higher momentum (it has not gone through the reversing flow process). Fluids flowing over these regions, including those over region IV, are forced to flow toward, and diagonally over, the suction surface by the transvers flow of region VI (cf. Fig. 5). These tubes of fluids, depending on their momentum, may maintain their identity for some distance downstream or may disappear (cf. Fig. 3). Some of them turn into vortices, or are taken over by neighboring vortices [6]. Between vortices of compatible strength, but incompatible rotation, new vortices are formed.

Over region VII, a complex system of vortices also develops; these are collectively called corner vortices. Figure 5 shows the imprint of these vortices as visualized [8] and measured via mass transfer [7]. These vortices have their origins in the diversion of upstream fluid to flow over the suction side. The upward flow of the fluid in

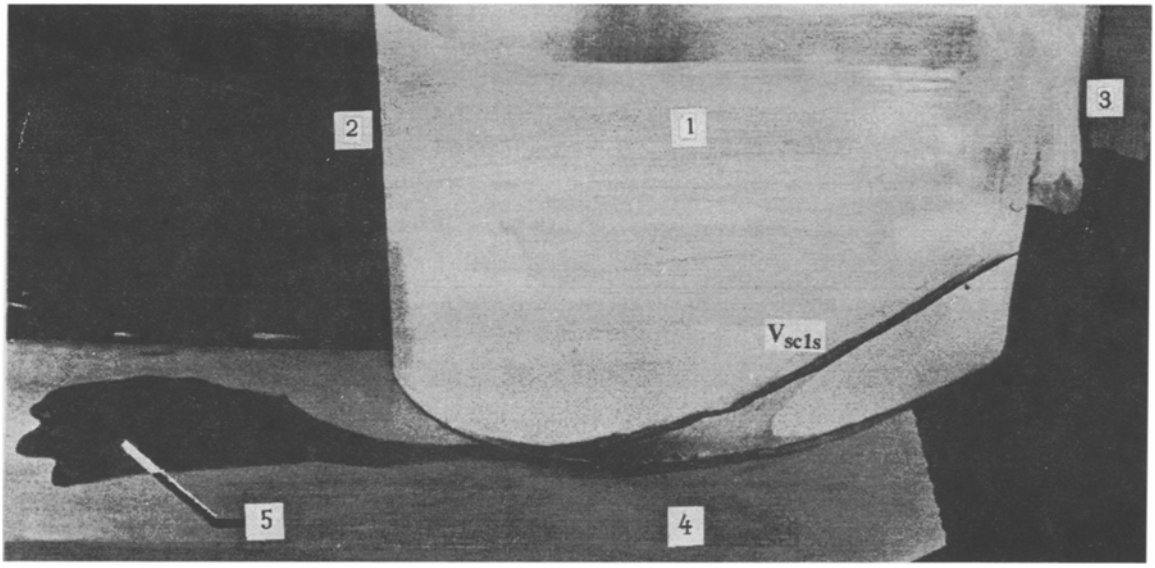

Fig. 5. Visualization of the path of vortex Vscls.

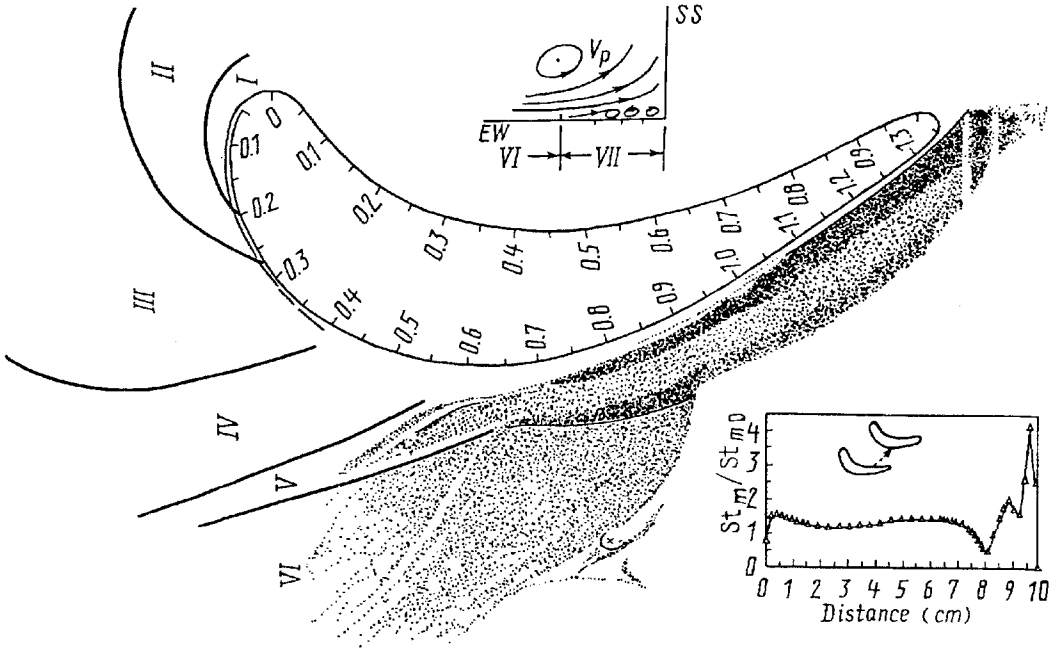

Fig. 6. Corner vortices as visualized and sensed via changes in mass transfer.

region VI near the blade/endwall (Fig. 6), and the detachment of the flow in region VII from the suction side, may also be contributing factors.

CONCLUSIONS

Measured film cooling effectiveness and mass transfer coefficients, supported by surface-flow visualization, indicate that the near-endwall-region of the passage between turbine blades is dominated by a complex flow system. This flow includes several flow tubes and vortices of which the two prominent ones are the horseshoe and the passage vortices. Most of the fluid in the layer immediately above regions I-IV (Fig. 4), save for a little that may be drawn into corner vortices, are pushed into tubes that flow over the region B of the suction surface (Fig. 2). Consequently, any film cooling fluid injected into the boundary layer over these regions is not going to benefit the

downstream sections of the endwall (regions V, VI, and VII), or the near endwall region of the suction side (region C). Some of the flow of region A (with higher concentration of injectant) is drawn over region B due to the direction of rotation of the suction-side leg of the horseshoe vortex. This may be one reason for the reduction of effectiveness in region B as region C is approached. Film cooling protection of regions VI and C appear to be possible only by injection either in region VI or region VI and region C, respectively.

The vortices in region VII on the endwall, and in regions B and C on the suction surface, are primarily responsible for abrupt changes in mass transfer coefficient in these areas. The local maxima and minima appear to correspond to the boundaries between adjacent flow tubes (wash-down and wash-up sections between pairs of counter rotating vortices). The interrupted length of strips over which the local maxima or minima occur indicates that some of these vortices (or flow tubes) form at some point, last over a distance, and disappear downstream. Further information on the appearance, endurance, and disappearance of these vortices is needed to enable their prediction and management of their effects.

NOTATION

C, cord length; D, injection hole diameter; DL, flow dividing line; H, blade's height from the endwall; M, blowing rate; Re_D, Reynold's number based on D; S_s, distance along suction side from the leading edge; St_m, mass transfer Stanton number; St_{m0}, mass transfer Stanton number on the endwall in the absence of the blades; X, distance along suction side from downstream edge of the injection holes.

REFERENCES

1. E.R.G. Eckert, "Analogies to heat transfer processes", in: Measurements in Heat Transfer (edited by E.R.G. Eckert and R.J. Goldstein), Hemisphere Publishing Co., New York (1976).
2. R.C. Hain, H.P. Wang, P.H. Chen, and R.J. Goldstein, "A microcomputer-controlled data acquisition system for naphthalene sublimation measurement", Proc. 11th ABCM Mech. Eng. Conf. (Sao Paulo, December, 1991) Brazil (1991).
3. R.J. Goldstein and H.P. Chen, "Film cooling on a gas turbine blade near the endwall", J. Eng. Gas Turbines and Power, 107, 117-122 (1985).
4. R.J. Goldstein and H.P.Chen, "Film cooling of a turbine blade with injection through two rows of holes in the near-endwall region", ASME Paper 87-GT-196 (1987).
5. H.P. Chen and R.J. Goldstein, "Convective transport phenomena on the suction surface of a turbine blade including the influence of secondary flows near the endwall", ASME Paper 91-GT-35 (1991).
6. M.Y. Jabbari, R.J. Goldstein, K.C. Marston, and E.R.G. Eckert, "Three-dimensional flow at the junction between a turbine blade and endwall", Z. Wärme-und Stoffübertragung (Thermo- and Fluid Dynamics), 27, No. 1 (1992).
7. R.J. Goldstein and R.A. Spores, "Turbulent transport on the endwall in the region between adjacent turbine blades", J. of Heat Transfer, 110, 862-869 (1988).
8. M.Y. Jabbari and R.J. Goldstein, "Visualization of flow in the endwall region of a turbine cascade", in: Atlas of Visualization, Vol. 1 (1992).